Carbohydrate Polymers 78 (2009) 488–491

Contents lists available at ScienceDirect

Carbohydrate Polymers

journal homepage: www.elsevier.com/locate/carbpol

Study on the interfacial properties of viscous capillary flow of dilute acetic acid solutions of chitosan

Zhengchun Cai [a], Jie Dai [a], Hu Yang [a,*], Rongshi Cheng [a,b,*]

[a] Key Laboratory of Mesoscopic Chemistry of MOE, School of Chemistry and Chemical Engineering, Nanjing University, Nanjing 210093, PR China
[b] College of Material Science and Engineering, South China University of Technology, Guangzhou 510641, PR China

ARTICLE INFO

Article history:
Received 22 February 2009
Received in revised form 27 March 2009
Accepted 11 May 2009
Available online 18 May 2009

Keywords:
Chitosan
Interfacial properties of viscous capillary flow
Solute adsorption effect

ABSTRACT

The relative viscosities of acetic acid solutions of chitosan at varied temperatures were measured in a common glass capillary Ubbelohde viscometer in the range from dilute down to extremely dilute concentration. With the aid of the newly proposed theory related to the effect of solute adsorption on the relative viscosity measurement, the experimental data was analyzed, and some interesting parameters describing the interfacial properties of viscous capillary flow were deduced. The change of the conformation of the chitosan chains both free dissolved in solution and adsorbed on the glass capillary surface were discussed in detail. Furthermore, the morphologies of the adsorbed chitosan was also observed by AFM.

© 2009 Elsevier Ltd. All rights reserved.

1. Introduction

The conformation of the adsorbed polymers layer on the solid surface has been kept an interesting topic, since it could affect many technical processes and problems (Fleer, Cohen, Scheutjens, Gasgove, & Vincent, 1993; Kawaguchi & Takahashi, 1992). For example, cardiovascular diseases have been paid more attention recently, it is believed that one of the reasons for causing this disease is that the adsorbed protein molecules on the wall of the capillary vessel would block the hemal flow, and result in the increase of blood pressure (Levy & Moskowitz, 1982). However, experimentally, the hydrodynamic method is believed a simple method to study on the interfacial properties of viscous capillary flow (Cheng, Shao, Liu, & Qian, 1998). Recently, Cheng et al. (Cai, Bo, & Cheng, 2005; Cheng, 1997; Cheng, Yang, & Yan, 1999) developed a new theory regarding the wall effect in the viscometry of polymer solutions, which further investigated the interfacial properties of capillary flow. This theory also reasonably explained the abnormalities viscosity behaviors of polymers in extremely dilute solutions, such as the upward or downward bending phenomenon of a curve of the reduced viscosity versus the concentration. The phenomena was always considered as experimental errors and ignored by previous researchers. However, Cheng et al. (Cai et al., 2005; Cheng, 1997; Cheng et al., 1999) believed that the cause of the abnormalities viscosity behaviors were not experimental errors, but should be ascribed to the wall effect of the capillary flow. Furthermore, based on this theory, some interesting interfacial information, such as the adsorption amount and the effective adsorbed layer thickness on the glass capillary surface, could be deduced. According to this rule, the relative viscosities of neutral polymers, synthetic polyelectrolytes and some amphoteric biomacromolecules (Li, Cai, Zhong, & Cheng, 2008; Li & Cheng, 2006; Yang, Yan, & Cheng, 1999) solutions from dilute to the extremely dilute concentration were measured, respectively, and interfacial properties of the capillary flow of polymer solutions mentioned above were investigated.

Chitosan is one of the well-known polysaccharides, and is partially deacetylated derivative of chitin, which is the second most abound natural polymers in the world. In acidic media, chitosan is converted to polyelectrolyte because of the protonization of the $-NH_2$ group on the C-2 position of the D-glucosamine repeat unit (Rinaudo, 2006). As one of high-performance natural polymer materials, it has been widely studied and applied in different fields especially in the biomedical and pharmaceutical industries (Mathias, 2006; Ravi Kumar, Muzzarelli, Muzzarelli, Sashiwa, & Domb, 2004; Thanou & Junginger, 2005). However, there was few report related to the interfacial properties of capillary flow of dilute acetic acid solutions of chitosan. In present work, the relative viscosities of dilute acetic acid solutions of chitosan with different concentrations were measured in a temperature range from 15 to 45 °C, and the results were analyzed on the basis of a theoretical representation of the solute adsorption effect on the viscosity measurement proposed by Cheng et al. (Cai et al., 2005; Cheng, 1997; Cheng et al., 1999). Furthermore, the morphologies of the chitosan on the glass surface were also observed by AFM.

* Corresponding authors. Tel.: +86 25 83686350; fax: +86 25 83317761 (H. Yang).
E-mail addresses: yanghu@nju.edu.cn (H. Yang), rscheng@nju.edu.cn (R. Cheng).

0144-8617/$ - see front matter © 2009 Elsevier Ltd. All rights reserved.
doi:10.1016/j.carbpol.2009.05.009

2. Experimental

2.1. Materials

The chitosan sample used in present work was commercial product purchased from Shandong AK Biotech Ltd. with degree of deacetylation about 90.5% quoted by the manufacturer. The viscosity average molecular weight, $M\eta = 2.96 \times 10^5$ g/mol, was estimated from the intrinsic viscosity determined in the solvent of 0.1 M CH_3COONa/0.2 M CH_3COOH using the Mark–Houwink parameters: $\alpha = 0.88$, $K = 6.589 \times 10^{-3}$ mL/g at 30 °C (Wang, Bo, Li, & Qin, 1991; Wang, Qin, & Bo, 1991).

2.2. Viscosity measurement

A stock solution of the chitosan was freshly prepared by weighing and dissolving in 1% acetic acid solution at room temperature (Rinaudo, Pavlov, & Desbrières, 1999). The de-ionized water was used in all experiments. The viscosity measurements were carried out using an Ulldeband-type capillary viscometer with the diameter and length of 0.40 mm and 10.0 cm, respectively. The measured temperature from 15 °C to 45 °C (±0.01 °C) was controlled well by a circulating water bath. The solutions were filtered by a Millipore filter with 0.45 μm pore-diameter to remove dust before any measurements. Firstly, a known weight of solvent (1% acetic acid solution) was transferred into the viscometer, and its efflux time t_v was measured carefully. Then, a definite amount of stock sample solution with a known weight concentration was added into the viscometer by weighing successively until the relative viscosity reached a predetermined point, in order to increase the solution concentration in the viscometer. The weight concentration was converted into a weight–volume concentration (in g/mL) by applying density corrections to the solution. The efflux time t_u for each solution with different concentration in the viscometer were measured. The ratio of flow time of solution to that of solvent, t_u/t_v, was regarded as the relative viscosity.

2.3. Dynamic light scattering (DLS)

Hydrodynamic diameters D_h of the chitosan particles in 1% acetic acid solution with a concentration of 3.0×10^{-4} g/mL were determined by dynamic light scattering model of Brookheaven BI200SM at varied temperatures. Uniphase *He–Ne* laser ($\lambda_o = 532$ nm) as the light source was used, and scattering angle was 90°. All analyses based on CONTIN procedure were triplicated with each run of 3 min, and the final results were the average of three runs.

2.4. Atomic force microscopy (AFM)

AFM (SPI3800, Seiko Instruments Inc, Japan) was used to study the morphologies of the adsorbed chitosan on the glass surface. One clean glass slide was vertically dipped in a chitosan/1% acetic acid solution with the concentration of 3.0×10^{-4} g/mL repeatedly, which simulated the viscous flow of polymer solutions in the capillary. Then, the treated glass slide was dried under nitrogen atmosphere at room temperature for further AFM observation. AFM measurement was performed with a 20-mm scanner in tapping mode.

3. Results and discussion

Fig. 1 showed the approximate linear dependence of experimental relative viscosity $\eta_{r,exp}$ of acetic acid solutions of chitosan versus the concentration at varied temperatures. Based on the results shown in Fig. 1, the curves of the relations between reduced viscosity and concentration were measured and shown in Fig. 2.

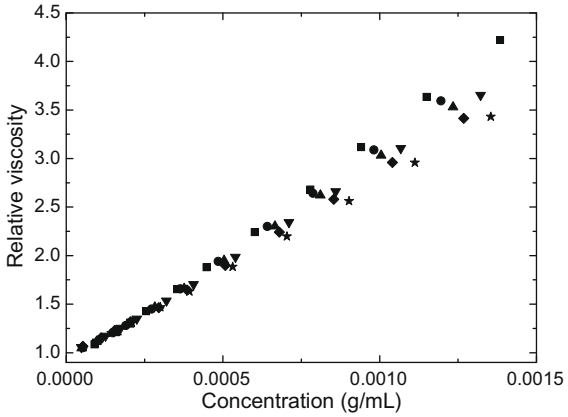

Fig. 1. Relative viscosity of acetic acid solutions of chitosan versus concentration at varied temperatures: (■) 15 °C, (●) 20 °C, (▲) 25 °C, (▼) 30 °C, (♦) 35 °C, (★) 45 °C.

From Fig. 2, it appeared down-bending shape in the extremely dilute concentration region at each temperature. Thus, the traditional theory of calculating the intrinsic viscosity [η] by extrapolating the concentration to zero according to Huggins equation was not suitable. It was proved that the wall effect on the viscosity measurement resulted in the viscosity abnormities in the extremely dilute concentration region (Cai et al., 2005; Cheng, 1997; Cheng et al., 1999). Since the solute were facilely adsorbed onto the glass capillary surface of the viscometer, the solute adsorption reduced the radius of capillary of viscometer, on the other hand, the actual concentration of the solution was also decreased, which both affected the viscosity measurement. At higher concentration range, the amount of adsorbed polymer on the glass capillary surface is much smaller than the residue, so adsorption effects on the viscosity measurement could be ignored. But, at the extremely dilute concentration range, the both effects mentioned above were much more markedly, and should be considered in the measurement.

Cheng et al. (Cai, Bo, & Cheng, 2003; Cai et al., 2005; Cheng, 1997) proposed the theory for describing the effect of solute adsorption on relative and reduced viscosity measured under viscous flow mode, the formulas, based on above two effects: the reduction of the radius of the viscometer capillary and the decrease

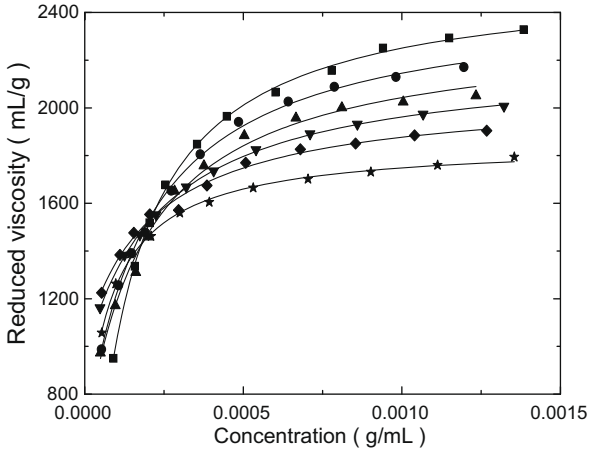

Fig. 2. Reduced viscosity of acetic acid solutions of chitosan versus concentration at varied temperatures: (■) 15 °C, (●) 20 °C, (▲) 25 °C, (▼) 30 °C, (♦) 35 °C, (★) 45 °C. The thin solid lines represent the theoretic simulated curves based on Eqs. (1) and (2) (see text).

of the solution concentration, both due to solute adsorption, were shown in Eqs. (1) and (2), respectively.

$$\eta_{r,exp} = (1 + [\eta] \cdot C + 6 \cdot K_m \cdot [\eta] \cdot C^2) \cdot \left(1 + k \cdot \frac{C}{C_a + C}\right) \quad (1)$$

$$C = C_0 \cdot \left(1 - \frac{A}{(C_a + C_0)}\right) \quad (2)$$

where $[\eta]$ is the intrinsic viscosity and K_m is self-association constant of polymer chains in solution and numerically correlates with the Huggins coefficient k_H and intrinsic viscosity $[\eta]$ as (Pan & Cheng, 2000):

$$K_m = \frac{1}{6} \cdot k_H[\eta] \quad (3)$$

Parameter k is defined as the fractional increment of flow time of solvent through the capillary saturated with adsorbed polymer compared with that of solvent through the clean bare capillary, and C_a is a characteristic concentration at which the surface coverage of the adsorbed polymer equals to 1/2. A is a constant related to the absorption capacity and C_0 is the initial concentration of solution. In the case of polymer adsorption, an effective adsorbed layer thickness b_{eff} could be deduced from parameter k as

$$b = R \cdot (1 - (1 + k)^{-\frac{1}{4}}) \quad (4)$$

where R is the radius of capillary in viscometer.

The experimental data of chitosan solution were analyzed further with the aid of the above theory. According to Eqs. (1) and (2), the reduced viscosity data were treated by an iterative fitting procedure; Since chitosan would be converted to a cationic polyelectrolyte after dissolved in acidic media, the inter-chain aggregations was absent in the dilute solution because of the coulomb repulsion force, which resulted in the values of K_m equal to zero during all measured temperature ranges, because the parameter of K_m described the degree of inter-chain aggregations in solution. Then, the experimental data of reduced viscosity were simulated by above theory. From Fig. 2, it was found that the theoretic simulated curves as thin solid lines fitted the experimental data in a fairly good way at each temperature, which indicated that this theory was also applicable to the natural polymers. And the simulated parameters such as K_m, C_a, k, A, and $[\eta]$ were summarized in Table 1.

The temperature dependence of the simulated intrinsic viscosity $[\eta]$ was shown in Fig. 3, it was found that $[\eta]$ decreased with temperature increase. Furthermore, Hydrodynamic diameters D_h of chitosan at each temperature were also measured by DLS, and listed in Table 1 and also shown in Fig. 3. It indicated clearly that the regularity of size change for chitosan chain in acetic acid solution, with temperature increase, was fully consistent with that of the intrinsic viscosity $[\eta]$, which may be ascribed to the decrease of the stiff conformation of chitosan in solution with temperature increase.

Interestingly, from Fig. 4, it could be found that the temperature effects on the values of parameter A and the effective adsorbed layer thickness b_{eff} were not linear as expected: with the temperature increase, both increase firstly, and after reaching the maximum around 20 °C, then decreased, which indicated that the amount of adsorption on the glass capillary surface of viscometer changed with temperature, and the largest amount occurred around 20 °C. But, based on Fig. 3, the size of the chitosan chains linearly decreased with temperature increase. So it is believed that, besides the conformation of the free chitosan chain dissolved in solution changed with temperature, that of the adsorbed chitosan layer on the glass capillary surface also changed. At dilute concentration region, the chitosan chain kept isolated state in solution, and the intra-chain hydrogen bond was dominated at lower temperature, which made the local chain quite stiff (Wang, Bo, & Qin, 1990; Wang, Bo et al., 1991; Wang, Qin et al., 1991). So chitosan chain showed extended conformation, and the adsorbed chain on the glass capillary was almost flatten on the surface, which resulted in a larger contact area on the capillary surface taken up by one adsorbed polymer chain, so the parameter A and effective adsorbed layer thickness b_{eff} lay in a lower level. With the temperature increase, the intra-chain hydrogen bond was broken gradually, and the stiffness of polymer chains decreased,

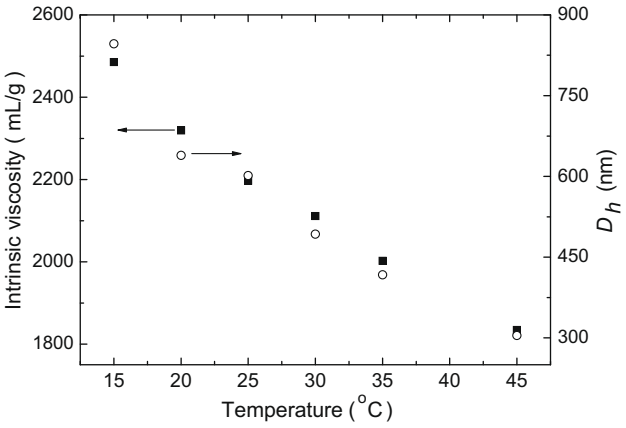

Fig. 3. Plots of the intrinsic viscosity $[\eta]$ and hydrodynamic diameter D_h versus the temperature. (■) $[\eta]$, (○) D_h.

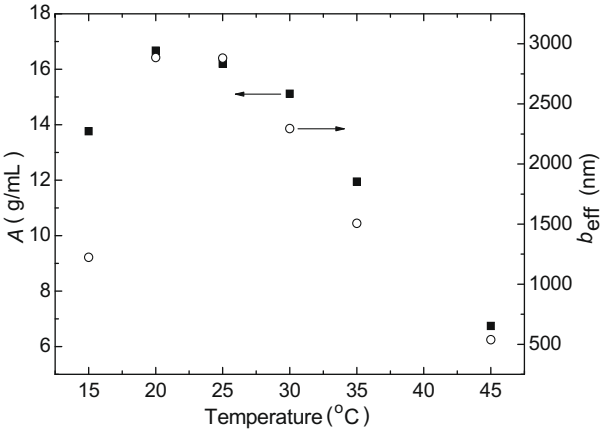

Fig. 4. Plots of the absorption capacity parameter A and the effective adsorbed layer thickness b_{eff} versus the temperature. (■) A, (○) b_{eff}.

Table 1
Summary of different parameters for chitosan in 1% acetic acid solutions at varied temperatures.

Temperature (°C)	$[\eta]$ (mL/g)	$K \times 10^3$	$A \times 10^5$ (g/mL)	$C_a \times 10^5$ (g/mL)	K_m	b_{eff} (nm)	D_h (nm)
15	2486	24.84	13.77	12.37	0	1223	846.5
20	2320	59.85	16.67	21.71	0	2885	639.2
25	2197	59.76	16.20	21.41	0	2881	601.6
30	2111	47.24	15.12	15.83	0	2295	492.7
35	2002	30.71	11.95	13.10	0	1507	417.0
45	1834	10.82	6.74	9.76	0	537	304.4

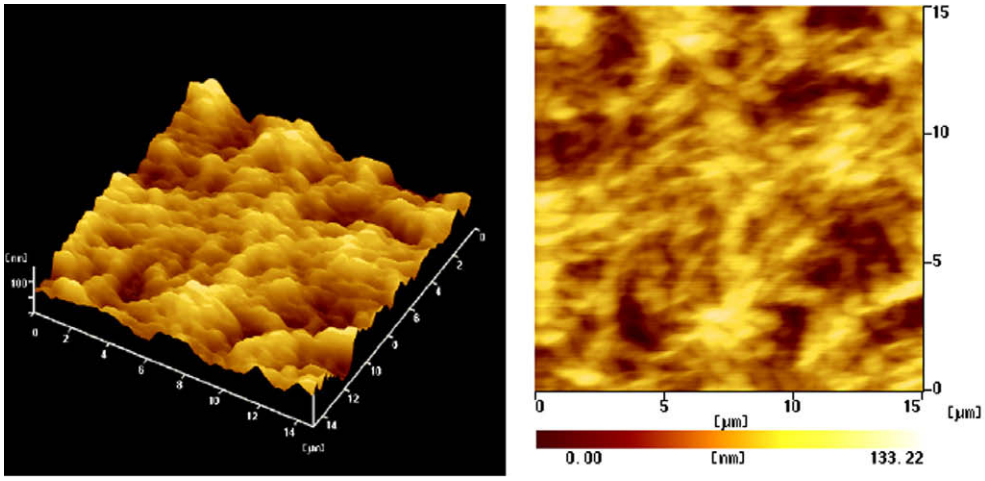

Fig. 5. AFM images of chitosan adsorption morphologies on the glass surface.

which led to the size of chain decrease as shown in Fig. 3; On the other hand, the conformation of the adsorbed chitosan on the capillary turned from flatten to crouched, and the contact area of one adsorbed chain on the surface also decreased, which made more polymers adsorbed on the capillary, so the actual adsorbed amount increased further. Furthermore, the stiffness decrease of chitosan chain as temperature increases causing by the intra-chain hydrogen bond broken was also supported by previous experimental facts of ^{1}H NMR (Brugnerotto, Desbrieres, Heux, Mazeau, & Rinaudo, 2001). However, when the temperature increased further, the Brownian motion of the polymers was more active, and some adsorbed chitosan on the glass surface were desorbed, so the parameter A and b_{eff} decreased again as shown in Fig. 4. In addition, from the Table 1, the change trend of the parameters k and C_a also supported this viewpoint.

Atomic force microscopy imaging provided further evidence for the adsorption morphology of chitosan on the glass surface. As seen from images shown in Fig. 5, the chitosan chains spread out on the surface with an average thickness around 100 nm. Comparison to the calculated effective adsorbed layer thickness b_{eff} listed in Table 1, the direct observed thickness by AFM was much smaller, which may be ascribed to lying in different state of samples: in solution and in dry state, respectively.

Another interesting fact was the downward bending phenomenon of the curves of the reduced viscosity of chitosan versus the concentration in extremely dilute solution region as shown in Fig. 2. Based on the above discussion, the effect of solute adsorption was concluded to explain the abnormalities viscosity behaviors of chitosan solution. But, according to previous work (Cai et al., 2005; Cheng, 1997; Cheng et al., 1999), the effect of solute adsorption usually made the upward bending phenomenon of the reduced viscosity curves, not downward bending, and downward bending phenomenon was usually explained by the effect of slip flow. However, in terms of the two opposite effects on the viscous flow mentioned above: the reduction of the radius of the viscometer capillary and the decrease of the solution concentration due to the adsorbed solute on the glass capillary surface, the former effect was usually more significantly, which made the upward bending phenomenon of the reduced viscosity curves; On the contrary, the downward bending phenomenon appeared. In this case, it was believed that the later effect was dominated in the extremely dilute concentration region for the stiff conformation of chitosan, so the downward bending phenomenon of the curves of reduced viscosity versus concentration were observed.

4. Conclusion

Based on the newly developed theory (Cai et al., 2005; Cheng, 1997; Cheng et al., 1999), the interfacial properties of viscous capillary flow of chitosan in 1% acetic acid solution were investigated. Although there were different temperature dependences of the respective parameters describing the structure states of the chitosan chains free dissolved in solution and adsorbed on the glass capillary surface, they bear the same intrinsic factor that was the stiff conformation of chitosan chains decreased, which was resulted from intra-chain hydrogen bond broken gradually with temperature increase.

Acknowledgement

This work was supported by the Key Nature Science Foundation of China (50633030).

References

Brugnerotto, J., Desbrieres, J., Heux, L., Mazeau, K., & Rinaudo, M. (2001). *Macromolecular Symposia, 168*, 1–20.
Cai, J. L., Bo, S. Q., & Cheng, R. S. (2003). *Colloid Polym. Sci., 82*, 182–187.
Cai, J. L., Bo, S. Q., & Cheng, R. S. (2005). *Polymer, 46*, 10457–10465.
Cheng, R. S. (1997). In D. B. Zhu & L. H. Shi (Eds.), *Polymers and organic solids* (pp. 69–78). Beijing: Science Press.
Cheng, R. S., Shao, Y. F., Liu, M. Z., & Qian, R. Y. (1998). *Eur. Polym. J., 34*(11), 1613–1619.
Cheng, R. S., Yang, Y., & Yan, X. H. (1999). *Polymer, 40*, 3773–3779.
Fleer, G., Cohen, S. M., Scheutjens, J., Gasgove, T., & Vincent, B. (1993). In *Polymer at interfaces*. London: Chapman and Hall.
Kawaguchi, M., & Takahashi, A. (1992). *Adv. Colloid Interface Sci., 37*, 219–317.
Levy, R., & Moskowitz, J. (1982). *Science, 217*, 121–129.
Li, Y., Cai, Z. C., Zhong, W., & Cheng, R. S. (2008). *J. Appl. Polym. Sci., 107*(3), 1850–1856.
Li, Y., & Cheng, R. S. (2006). *J. Polym. Sci. Part B: Polym. Phys., 44*(13), 1804–1812.
Mathias, U. (2006). *Polymer, 47*(7), 2217–2262.
Pan, Y., & Cheng, R. S. (2000). *Chin. J. Polym. Sci., 8*(1), 57–67.
Ravi Kumar, M. N. V., Muzzarelli, R. A. A., Muzzarelli, C., Sashiwa, H., & Domb, A. J. (2004). *Chem. Rev., 104*, 6017–6084.
Rinaudo, M. (2006). *Prog. Polym. Sci., 31*, 603–632.
Rinaudo, M., Pavlov, G., & Desbrières, J. (1999). *Polymer, 40*(25), 7029–7032.
Thanou, M., & Junginger, H. E. (2005). In S. Dumitriu (Ed.), *Polysaccharides. Structural diversity and functional versatility* (2nd ed., pp. 661–677). New York: Marcel Dekker Publ.
Wang, W., Bo, S. Q., Li, S., & Qin, W. (1991). *Int. J. Biol. Macromol., 13*(5), 281–285.
Wang, W., Bo, S. Q., & Qin, W. (1990). *Sci. China Ser. B Chem., 11*, 1126–1131.
Wang, W., Qin, W., & Bo, S. Q. (1991). *Makromol. Chem. Rapid Commun., 12*(9), 559–561.
Yang, Y., Yan, X. H., & Cheng, R. S. (1999). *J. Macromol. Sci. Phys., B38*(3), 237–249.